

ALKALI ATTACK OF COAL GASIFIER REFRACTORY LINING

by

Maria Gentile

Thesis submitted to the Graduate Faculty of the
Virginia Polytechnic Institute and State University
in partial fulfillment of the requirements for the degree of

MASTER OF SCIENCE

in

MATERIALS ENGINEERING

APPROVED:

J. J. Brown, Jr., Chairman

R. H. Yoon

D. Farkas

ALKALI ATTACK OF COAL GASIFIER REFRACTORY LINING

by

Maria Gentile

Committee Chairman: Jesse J. Brown

Materials Engineering

(ABSTRACT)

An experimental test system was designed to simulate the operating conditions found in nonslagging coal gasifiers. The reaction products that form when refractory linings in coal gasifiers are exposed to alkali impurities (sodium or potassium) were experimentally determined. Analysis of selected physical and chemical properties of the reaction products, which typically form between the alkali and the refractory will lead to a better understanding of the mechanisms behind refractory failures associated with alkali attack.

The reaction products sodium aluminate ($\text{Na}_2\text{O}\cdot\text{Al}_2\text{O}_3$), $\text{N}_2\text{C}_3\text{A}_5$ ($2\text{Na}_2\text{O}\cdot 3\text{CaO}\cdot 5\text{Al}_2\text{O}_3$), nepheline ($\text{Na}_2\text{O}\cdot\text{Al}_2\text{O}_3\cdot 2\text{SiO}_2$), potassium aluminate ($\text{K}_2\text{O}\cdot\text{Al}_2\text{O}_3$), and kaliophilite ($\text{K}_2\text{O}\cdot\text{Al}_2\text{O}_3\cdot 2\text{SiO}_2$) were synthesized and their solubility in water and coefficients of linear thermal expansion were measured. Of the compounds tested, the formation of potassium aluminate would be the most detrimental to the gasifier lining. The linear thermal expansion of potassium aluminate was 2.05% from room

temperature to 800°C , which was twice as large as the other compounds. Potassium aluminate also possessed the highest solubility in water which was 8.89g/L at 90°C .

Acknowledgements

I would like to thank Dr. J. J. Brown, Jr. for his guidance and patience throughout my graduate studies in Materials Engineering. To Nancy Brown for her editorial assistance.

I would also like to thank Dr. Farkas and Dr. Yoon for serving on my committee. To _____ and _____ for their help and guidance throughout my stay in Blacksburg.

Table of Contents

	<u>Page</u>
Abstract	ii
Acknowledgements	iv
I. Introduction	1
A. Background Information	1
B. Alkali Attack of Alumino-Silicate Refractories	3
1. Reactions with Sodium	3
2. Reactions with Potassium	4
C. Alkali Attack of Calcium Aluminate Cements	4
1. Alkali-53% Alumina Cement Reactions	5
2. Alkali-71% Alumina Cement Reactions	8
II. Experimental Procedure	13
A. Test Apparatus	13
B. Alkali Compound Syntheses	13
C. Solubility Measurements	15
D. Thermal Expansion Measurements	16
III. Results and Discussion	18
A. Identification of Alkali-Alumina Cement Reaction Products	18
B. Solubility Results	24
C. Thermal Expansion Results	24
D. Discussion	34
IV. Conclusions	39
V. References	40
VI. Appendix I	42
VII. Appendix II	47
VIII. Vita	52

List of Tables

<u>Table</u>	<u>Page</u>
1. Composition of Gas Atmosphere (in mol%)	6
2. Composition of Alumina Cement (in mol%)	7
3. Calculated Equilibrium Phases and the Experimentally Observed Phases for the Sodium-53% Alumina Cement Reactions	19
4. Calculated Equilibrium Phases and the Experimentally Observed Phases for the Potassium-53% Alumina Cement Reactions	20
5. Calculated Equilibrium Phases and the Experimentally Observed Phases for the Sodium-71% Alumina Cement Reactions	22
6. Calculated Equilibrium Phases and the Experimentally Observed Phases for the Potassium-71% Alumina Cement Reactions	23
7. Coefficients of Linear Thermal Expansion of the Tested Alkali Compounds	35

List of Figures

<u>Figure</u>	<u>Page</u>
1. $\text{Na}_2\text{O}-\text{CaO}-\text{Al}_2\text{O}_3$ Phase Diagram	9
2. $\text{K}_2\text{O}-\text{CaO}-\text{Al}_2\text{O}_3$ Phase Diagram	10
3. Schematic of Test System	14
4. Solubility Curve for Sodium Aluminate	25
5. Solubility Curve for Soda-Lime-Aluminate	26
6. Solubility Curve for Nepheline	27
7. Solubility Curve for Potassium Aluminate	28
8. Solubility Curve for Kaliophilite	29
9. Thermal Expansion Curve for Sodium Aluminate	30
10. Thermal Expansion Curve for Soda-Lime-Aluminate	31
11. Thermal Expansion Curve for Nepheline	32
12. Thermal Expansion Curve for Potassium Aluminate	33
13. Thermal Expansion Curve for Kaliophilite	36

I. Introduction

A. Background Information

There are many industrial processes in which refractory structures are subjected to alkali vapors or slags. These structures include the linings of cement kilns and blast furnaces, much of the interior of glass tank furnaces, and coal gasifier linings. The result of combining the operating conditions of high temperature and pressure with alkali impurities (often in the presence of steam) is degradation and premature failure of the refractory structures. The Grand Forks Energy Technology Center (GFETC) slagging gasifier failure demonstrates the devastating effect alkali impurities may have on a refractory structure.⁽¹⁾ The mullite refractory lining in the gasifier cracked and spalled after only 125 hours of exposure in a coal gasification atmosphere. The mullite refractory was found to have reacted with sodium (probably NaOH) to form carnegiete ($\text{Na}_2\text{O} \cdot \text{Al}_2\text{O}_3 \cdot 2\text{SiO}_2$) and beta-alumina ($\text{Na}_2\text{O} \cdot 11\text{Al}_2\text{O}_3$). The failure occurred as a result of the volume expansion associated with this reaction. Chemical spalling due to reactions of mullite and alumina refractories with sodium compounds to form carnegiete (and its polymorphic variety, nepheline) and beta-alumina is a common problem. Analogs of these reactions have also been identified in the presence of potassium with leucite ($\text{K}_2\text{O} \cdot \text{Al}_2\text{O}_3 \cdot 4\text{SiO}_2$), kaliophilite ($\text{K}_2\text{O} \cdot \text{Al}_2\text{O}_3 \cdot 2\text{SiO}_2$) and beta-alumina ($\text{K}_2\text{O} \cdot 12\text{Al}_2\text{O}_3$) as reaction products.⁽²⁾ These products are formed as the alkali initially attacks the cristobalite and glass of the matrix bond, and then the fine crystalline mullite associated with bonding. Higher temperatures intensify the alkali attack of the coarser mullite. Free alumina is the most resistant component in the refractory

system. It is not readily attacked until all the available cristobalite, glass and mullite have reached equilibrium with the alkali. The reaction product formed from alkali and free alumina is beta-alumina, which is formed above 2000°F and exists up to approximately 3000°F⁽³⁾. The exact chemical composition of beta-alumina is still problematical. From chemical analysis a composition of $\text{Na}_2\text{O} \cdot 12\text{Al}_2\text{O}_3$ has been reported by a number of sources⁽⁴⁻⁵⁾. However a 1:11 ratio gives the best agreement with the crystal structure and density data. Two factors continue to influence this ratio: (1) the recognized difficulty of chemical analysis; and (2) the more recent possibility of more than one beta-alumina phase combined with nonstoichiometry dependent on the thermal history. Yamaguchi and Suzuki have identified another alkali polyaluminate by chemical analysis and x-ray methods and reported an approximate composition of $\text{Na}_2\text{O} \cdot 8\text{Al}_2\text{O}_3$ or $\text{K}_2\text{O} \cdot 8\text{Al}_2\text{O}_3$ ⁽⁶⁾. Higher concentrations of alkali will lead to the formation of alkali aluminates such as sodium aluminate ($\text{Na}_2\text{O} \cdot \text{Al}_2\text{O}_3$) or potassium aluminate ($\text{K}_2\text{O} \cdot \text{Al}_2\text{O}_3$). However, other factors besides reactivity must be considered in the resistance of a refractory to alkali attack.

Of the other factors to be considered, surface area is probably the most important. The extent of alkali attack is limited by access to the internal matrix of the refractory. Further resistance to alkali penetration is exhibited by the ability of some aluminous refractories to seal the surface by forming a glass (glazing). This leads, in general, to failure only if repetitive peeling of surface layers occurs. This peeling effect is often found in refractories exposed to cyclic

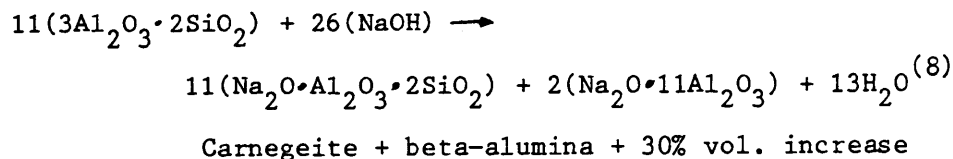
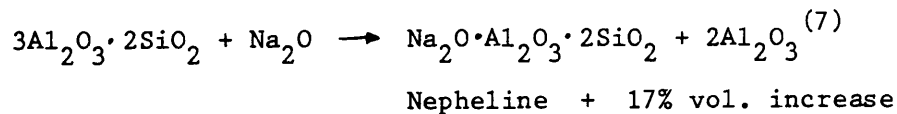
heating and cooling. In general, the alkali compounds tend to be hydrophylic when exposed to ambient atmospheric conditions, which results in rapid moisture removal and spalling when the alkali laden refractory structure is shut down then reheated. The alkali compounds also tend to have higher thermal expansion coefficients which makes the exposed surface layer more prone to thermal spalling upon subsequent heating and cooling.

B. Alkali Attack of Alumino-Silicate Refractories

When mullite or alumina refractories are exposed to alkali impurities (sodium or potassium), dry expansive type compounds form which are less dense than the parent refractory. Being less dense, the formation of alkali compounds will produce a volume expansion.

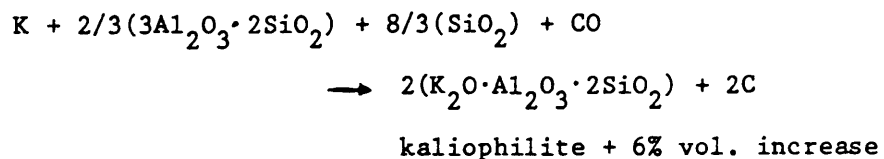
1. Reactions with Sodium

Nepheline and beta-alumina are the two most commonly formed alkali compounds in mullite structures. The formation of nepheline will result in a 17% volume expansion. A 20% volume increase is associated with the formation of beta-alumina. Two typical mullite-sodium reactions are shown below:

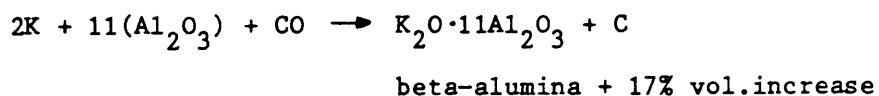
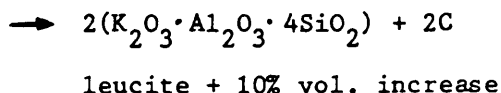


2. Reactions with Potassium

When potassium is present as the alkali impurity, kaliophilite (analogous to the sodium compound nepheline) or leucite are often the alkali compounds which form. The formation of kaliophilite will result in a 6% volume increase; while the formation of leucite will result in a 10% volume increase. A potassium form of beta-alumina is also observed in the alumina-potassia system with an accompanying 17% volume increase. (9)



or



C. Alkali Attack of Calcium Aluminate Refractory Cements

In the present investigation, the alkali attack of non-slugging coal gasifier refractory linings was studied. Alkali vapors are almost always present in coal gasifiers because feed coals contain alkali compounds. In general, the alkali attack is viewed as a long term phenomena, with the damage occurring over a period of many months or years of unit operation. Because gasifiers are frequently refractory lined, operated at high temperatures, and contain alkali impurities, it is important to study the reactions that occur and to evaluate the

results in view of design, operation, and lifetime of the refractory gasifier linings.

From a thermodynamic viewpoint, when refractories made from the $\text{CaO-Al}_2\text{O}_3\text{-SiO}_2$ system are exposed to alkali impurities, alkali reactions are inevitable, since the total energy of the system will be lowered by the formation of alkali compounds. The mechanism of alkali attack on coal gasifier linings consists of the release of the alkali species from the coal and the subsequent reactions with the gasifier linings. It is known that the reactions primarily take place at the cement bonding phase. The aggregate remains unreacted with the alkali impurity. This is attributed to the larger grain size and smaller surface area of the aggregates as compared to the cement bonding phase.

The computer program SOLGASMIX-PV has been used to calculate the stable phases that form under equilibrium conditions in a nonslagging coal gasifier.⁽¹⁰⁾ In the calculations, the thermodynamic system contained one gas mixture, one liquid solution, and various invariant solid phases. The liquid solution is assumed to be ideal, and all the solid phases occur as stoichiometric compounds. The simulated gas atmosphere used in the calculations is listed in Table 1. A 53% alumina and a 71% alumina cement were used in the calculations. The compositions of the cement are given in Table 2. The calculations of interest were carried out at ambient pressure and temperatures ranging from 1200K to 1800K.

1. Alkali-53% Alumina Cement Reactions

Tables 3 and 4 show the mineralogical change of a 53% alumina cement after exposure to an atmosphere containing sodium or potassium,

Table 1. Composition of Gas Atmosphere (in mol %)

H ₂	CH ₄	CO	CO ₂	H ₂ O	N ₂
12	18	17	12	20	20

Table 2. Composition of Alumina Cement (in. wt%)

	Al_2O_3	CaO	Fe_2O_3	SiO_2
Intermediate purity	53.5	40.5	1.6	4.4
High purity	71.5	27.9	0.17	0.16

respectively. After exposure to a sodium atmosphere, the primary phases formed were CaO and $\text{Na}_2\text{O}\cdot\text{Al}_2\text{O}_3$ at low temperatures. Above 1400K, CaO disappeared and $3\text{CaO}\cdot\text{Al}_2\text{O}_3$ formed. No sodium compounds formed above 1600K. In the potassium calculations, CaO and $\text{K}_2\text{O}\cdot\text{Al}_2\text{O}_3$ were the primary phases formed throughout the testing temperatures.

2. Alkali-71% Alumina Cement Reactions

Similar results were obtained for the 71% alumina cement reactions. The equilibrium phases predicted from the calculation under sodium and potassium atmospheres are shown in Tables 5 and 6.

In a sodium atmosphere, the primary phases were CaO and $\text{Na}_2\text{O}\cdot\text{Al}_2\text{O}_3$ at low temperatures. Above 1400K, CaO disappears and $3\text{CaO}\cdot\text{Al}_2\text{O}_3$ and $\text{CaO}\cdot\text{Al}_2\text{O}_3$ form. Again no sodium compounds formed above 1600K. In the potassium atmosphere, CaO and $\text{K}_2\text{O}\cdot\text{Al}_2\text{O}_3$ were the only phases which formed throughout the temperature range tested.

The above results were compared with existing phase diagrams for $\text{Na}_2\text{O}-\text{Al}_2\text{O}_3-\text{CaO}$ and $\text{K}_2\text{O}-\text{Al}_2\text{O}_3-\text{CaO}$ (see Figures 1 and 2); the compositions of the cements used in the calculations are labeled on the diagrams. According to the phase diagrams, the stable phases corresponding to the labeled compositions are likely to be CaO and $\text{Na}_2\text{O}\cdot\text{Al}_2\text{O}_3$ for Figure 1 and CaO and $\text{K}_2\text{O}\cdot\text{Al}_2\text{O}_3$ for Figure 2. In the calculations, the sodium and potassium input levels were fixed at 1 mol%. Higher amounts of alkali produce alkali aluminates of higher alkali contents; thus the 1:1 ratio alkali-alumina compounds rather than the beta-alumina type compounds formed.

Analysis of the physical and chemical properties of the reaction products, which typically form between the alkali and the refractory

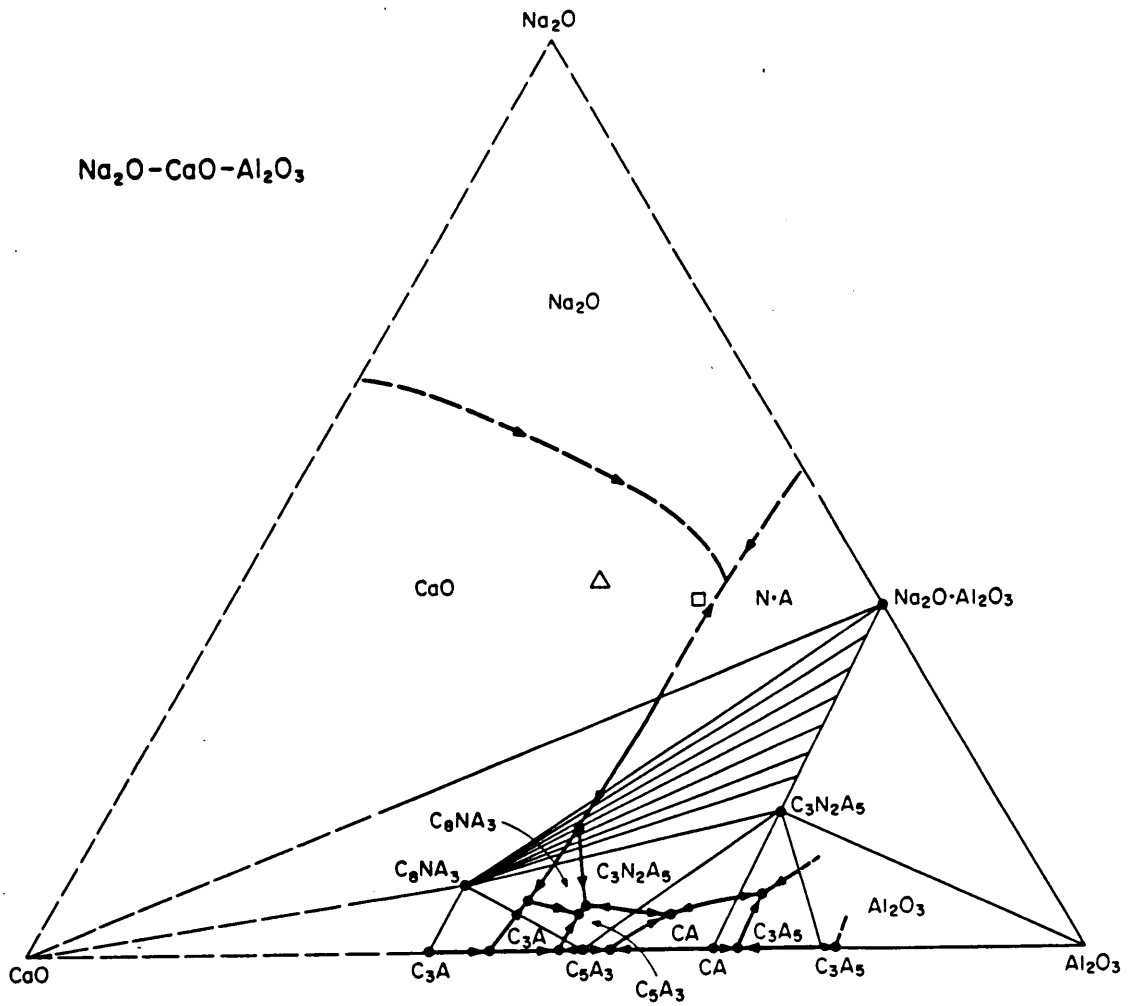


Figure 1. $\text{Na}_2\text{O}-\text{CaO}-\text{Al}_2\text{O}_3$ system. (Δ and \square represent compositions used in calculations for 53% and 72% alumina cement, respectively.)

will lead to a better understanding of the mechanisms behind the refractory failures associated with alkali attack. Of these properties, it is felt that dimensional changes, thermal expansion and water absorption are the most important. Sodium aluminate ($\text{Na}_2\text{O} \cdot \text{Al}_2\text{O}_3$), soda-lime-aluminate ($2\text{Na}_2\text{O} \cdot 3\text{CaO} \cdot 5\text{Al}_2\text{O}_3$), nepheline ($\text{Na}_2\text{O} \cdot \text{Al}_2\text{O}_3 \cdot 2\text{SiO}_2$), potassium aluminate ($\text{K}_2\text{O} \cdot \text{Al}_2\text{O}_3$), and kaliophilite ($\text{K}_2\text{O} \cdot \text{Al}_2\text{O}_3 \cdot 2\text{SiO}_2$) were the compounds chosen for physical and chemical testing.

In the ternary system soda-lime-alumina, the formation of $\text{N}_2\text{C}_3\text{A}_5$ is possible since its stability field is adjacent to the three basic calcium aluminate cement phases: C_{12}A_7 , CA, and CA_2 .⁽¹¹⁾ When the amount of Na_2O present is increased, sodium aluminate becomes the stable phase. The stability field of solid solutions of NA and $\text{N}_2\text{C}_3\text{A}_5$ lies between the stability field for $\text{N}_2\text{C}_3\text{A}_5$ and the single phase region where NA is stable; so at intermediate concentrations of Na_2O , both NA and $\text{N}_2\text{C}_3\text{A}_5$ are the stable equilibrium phases. X-ray diffraction studies have shown that the low-temperature tetragonal modification of sodium aluminate is converted to cubic form at 450°C .⁽¹²⁾ A characteristic feature of this polymorphic conversion is the constancy of the unit cell volumes, which are 2054 and 2058 \AA^3 for the low and high temperature forms respectively.

In the potassia-lime-alumina system, the field of $\text{K}_2\text{O} \cdot \text{Al}_2\text{O}_3$ is adjacent to C_3A , C_{12}A_7 , and CA and a eutectic is formed between C_3A , C_{12}A_7 , and KA at 1425°C .⁽¹¹⁾ Potassium aluminate crystallises in the cubic system with a refractive index of 1.603.

The compound $\text{Na}_2\text{O} \cdot \text{Al}_2\text{O}_3 \cdot 2\text{SiO}_2$ has four known polymorphs. High-carnegieite (cubic) is stable from the liquidus down to 1250°C ,

where it transforms to high-nepheline (hexagonal) which is stable down to room temperature. The transformation of high-carnegiete to high-nepheline is sluggish and, by quenching, high-carnegiete may be obtained in the stability field of nepheline but at 690°C it undergoes a displacive inversion into low-carnegiete (low symmetry).⁽¹³⁾

Five polymorphs of $K_2O \cdot Al_2O_3 \cdot 2SiO_2$ are known. Below 850°C, kalsite (hexagonal) is the stable phase. From 900°C to the liquidus, laboratory syntheses have yielded orthorhombic $KAlSiO_4$ (denoted 01); near 1000°C a synthetic kaliophilite with a hexagonal structure was also obtained. The synthetic kaliophilite is not identical to the natural kaliophilite which also has a hexagonal structure, but their powder patterns are remarkably similar. A second form of natural kaliophilite exists which is known as anomalous natural kaliophilite. Kaliophilite is analogous to the phase nepheline found in the soda-lime-alumina system. Both nepheline and kaliophilite exist in the hexagonal and the orthorhombic structural forms.

II. Experimental Procedure

A. Test Apparatus

The test apparatus shown in Figure 3 consists of a resistance heated tube furnace, a mechanical syringe pump, flow meters and a glass tube where the individual gases were premixed. The input gas composition (in mol%) was fixed at 12% H₂, 18% CH₄, 17% CO, 12% CO₂, 20% H₂O, and 20%N₂. The mechanical syringe pump was used to inject distilled water into the tube furnace at a constant rate of 0.3ml/hr. during testing. The furnace was operated at ambient pressure and temperatures ranging from 1200K to 1600K.

The alkali impurities were introduced by mixing sodium carbonate or potassium carbonate in a 1:1 weight ratio the calcium aluminate cement. The composition of the cements is given in Table 2. The ground sample was then fired in an alumina combustion boat for 30 hours in the gaseous atmosphere described above. At the completion of the run, the samples were removed at the testing temperature in an inert atmosphere. The samples were reground and sealed in plastic containers. The phase assemblage of each sample was identified by x-ray diffraction analysis.

B. Alkali Compound Syntheses

Sodium aluminate was formed by heating a stoichiometric mixture of sodium oxylate (Na₂C₂O₄) and aluminum hydroxide (Al(OH)₃) at 1000°C for 15 hours, after a preliminary heat of 600°C.⁽¹⁴⁾

Soda-lime-aluminate (2Na₂O·3CaO·5Al₂O₃) was synthesized by reacting sodium oxylate, calcium nitrate (Ca(NO₃)₂) and alumina powder in a 2:3:5 ratio. The mixture was heated at 1100°C for two days.

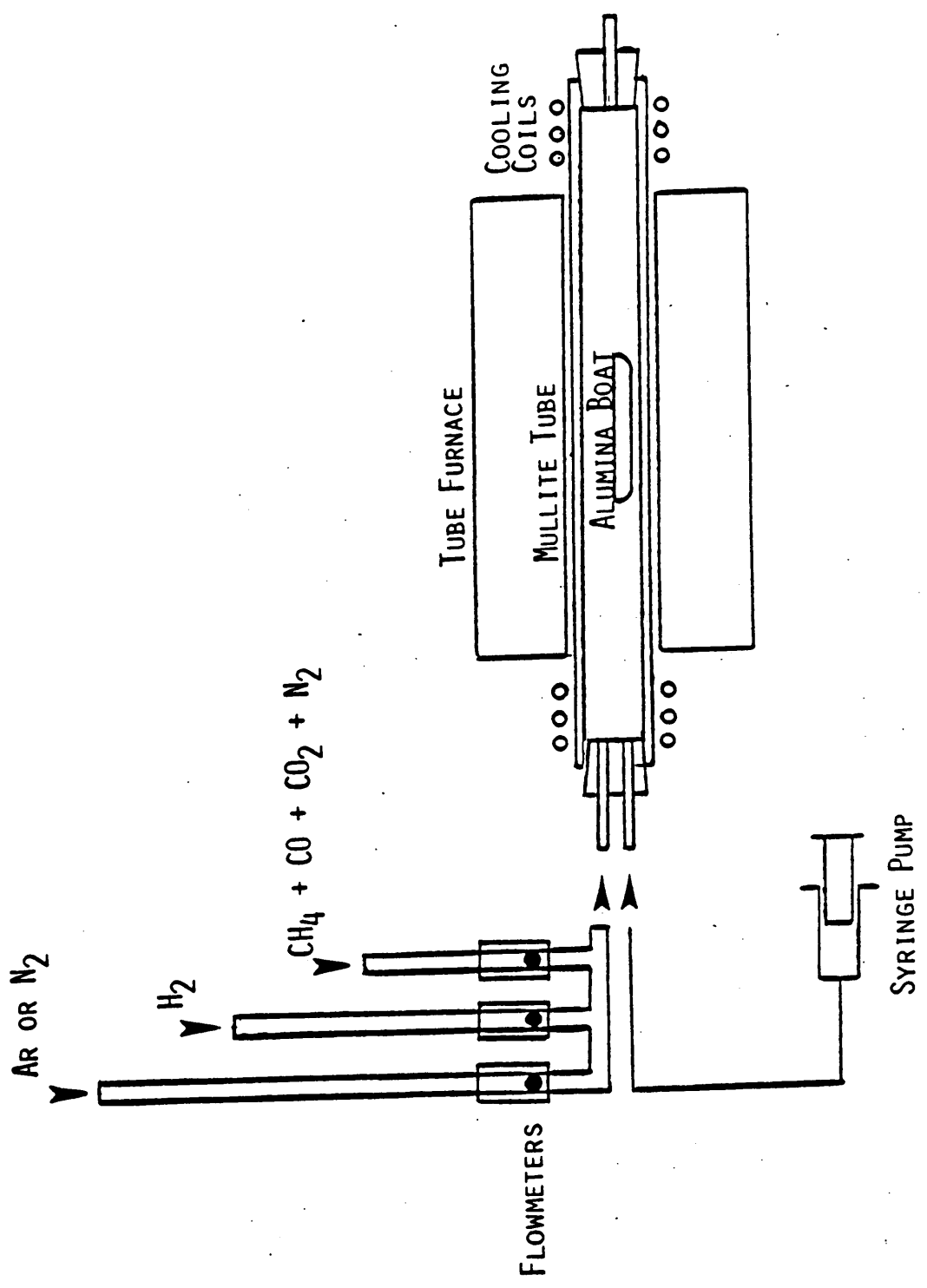


Figure 3. Schematic of Test System

Nepheline was prepared by reacting two moles of sodium hydroxide (NaOH) and one mole of kaolin ($\text{Al}_2\text{O}_3 \cdot 2\text{SiO}_2 \cdot \text{H}_2\text{O}$)⁽¹⁵⁾ at 1100°C for 4 days.⁽¹⁶⁾ Potassium aluminate was synthesized by reacting stoichiometric amounts of K_2O and Al_2O_3 in the form of K_2CO_3 and $\text{Al}(\text{OH})_3$. The mixture was heated in air at 1170K for 4 h; 870K for 64h; 1185K for 20.5h; 1185K for 5h; and 1185K for 25h. The mixture was cooled and thoroughly blended after each of the 1185K heatings.⁽¹⁷⁾

Kaliophilite was synthesized by reacting 2 moles of potassium hydroxide (KOH) and 1 mole of kaolin ($\text{Al}_2\text{O}_3 \cdot 2\text{SiO}_2 \cdot \text{H}_2\text{O}$). The mixture was heated for four days in air at 1100°C.

After the compounds were synthesized, x-ray powder diffraction analysis was performed to confirm that only the specified compounds were present. The compounds were immediately placed in sealed containers to prevent the absorption of moisture. The percent absorbed water was measured for each compound after the physical testing was completed. None of the compounds contained more than 0.15% absorbed water.

C. Solubility Measurements

Quantative determination of solubility consists essentially of two operations: the preparation of a saturated solution and its subsequent analysis. The most important consideration is the assurance that final equilibrium between solvent and solute has been reached. This is the point at which no further change occurs in the relationship between the amount of the compound in solution and that remaining undissolved. Only by thorough mixing which agitation or effective stirring provides can the point of saturation be reached with certainty. Since solubility is

a function of temperature, the temperature of the water must be accurately controlled when measuring solubility. In general, it may be stated, that every procedure designed for preparing a saturated solution must include provisions for accurate control of temperature and for active and continuous agitation or stirring of the solution.

To determine the solubility of the alkali compounds, saturated solutions were prepared in distilled water and mixed thoroughly with a magnetic stirrer. After a sufficient length of time for the attainment of saturation, the undissolved solid was allowed to settle. The clear solution was then collected with a pipet and the temperature and weight of the solution were recorded. The solution was then placed in a drying oven to remove all moisture. The remaining solid represents the amount of the compound that was soluble in the water. The solubility was calculated by dividing the weight of the dissolved solid by the volume of the distilled water. The procedure was performed at room temperature, 90°C and 5°C . Each solubility measurement was repeated four times. The values measured on successive trials were precise to one-hundredth of a gram per liter which is within the accuracy of the balance used to weigh the samples. All test conditions were kept constant to maintain the reproducibility of the measurements.

D. Thermal Expansion Measurements

To prepare the test samples for thermal expansion measurements, the compounds were finely ground and mixed with acetone. The powder was then pressed into $1/2''$ by $4''$ bars using a hydraulic press. Next the pressed bars were sintered at 1000°C for twenty-four hours. To measure the thermal expansion of the samples, the test bars were placed in a

fused quartz tube with a push rod centered on top of the sample. The push rod was connected to a Teclock dial gage capable of measuring dimensional changes to 0.001 of an inch. The samples were heated at a rate of 10°C/min. to 800°C in a tube furnace controlled by a variac power source. The coefficient of thermal expansion was calculated by measuring the dimensional change of the test bars in the direction of the longest dimension.

Thermal expansion curves were constructed for each of the compounds tested. The thermal expansion measurements were repeated three times and at the completion of each test the coefficient of thermal expansion was calculated and compared to the previously obtained values. The results obtained on successive trials differed by approximately 1% of the calculated mean value, indicating that the results were reproducible.

III. Results and Discussion

A. Identification of Alkali-Alumina Cement Reaction Products

The experimentally detected phases that formed between the alumina cement and alkali (sodium or potassium) were compared to the theoretically calculated stable, equilibrium phases reported by Sun.⁽¹⁰⁾

The 53% alumina cement-sodium phases are listed in Table 3. At 1200K, $C_{12}A_7$ ($12CaO \cdot 7Al_2O_3$) and sodium aluminate ($Na_2O \cdot Al_2O_3$) were the experimentally detected phases. According to the theoretical calculation, lime (CaO) and sodium aluminate are the stable phases. The loss of the lime phase is attributed to the formation of the nonequilibrium cement phase $C_{12}A_7$, which formed as a result of insufficient test time to allow equilibrium to be attained. At 1300K and 1400K, lime and sodium aluminate were the experimentally detected phases which agrees with the theoretical calculations. At higher temperatures (1500K and 1600K), lime and sodium aluminate were detected along with $N_2C_3A_5$. This can be explained by noting that at higher temperatures sodium is lost in the exit gas during testing; therefore, the composition of the sample drops into the region on the soda-lime-alumina diagram (see Figure 1) where $N_2C_3A_5$ is the stable phase.

The 53% alumina cement-potassium phases are listed in Table 4. At 1200K, $C_{12}A_7$ and potassium aluminate ($K_2O \cdot Al_2O_3$) were the experimentally detected phases. At 1300K and 1400K, lime and potassium aluminate were observed experimentally which agrees with the theoretical calculations. These results are very similar to those observed when sodium was

Table 3. Calculated Equilibrium Phases and the Experimentally Observed Phases for the Sodium-53% Alumina Cement Reactions*

Temperature (K)	Calculated	Observed
1200	C, NA	$C_{12}A_7$, NA
1300	C, NA	C, NA
1400	C, NA	C, NA
1500	C_3A , NA	C, NA, $N_2C_3A_5$
1600	C_3A , CA	C, NA, $N_2C_3A_5$

* Conventional cement chemistry notation used in Tables 3-6, i.e. C=CaO, N=Na₂O, A=Al₂O₃, K=K₂O.

Table 4. Calculated Equilibrium Phases and the Experimentally Observed Phases for the Potassium-53% Alumina Cement Reactions

Temperature (K)	Calculated	Observed
1200	C, KA	$C_{12}A_7$, KA
1300	C, KA	C, KA
1400	C, KA	C, KA
1500	C, KA	$C_{12}A_7$, CA
1600	C, KA	$C_{12}A_7$, CA

present as the alkali species. At 1500K and 1600K, the experimentally detected phases were $C_{12}A_7$ and CA. No potassium phases were detected. It is known that alkali vapors react aggressively with the calcium aluminate cement; however, our experimental apparatus allows the potassium to flow out of the tube furnace in the exit gas as it vaporizes. It should also be noted that only a finite amount of potassium is available during each testing. Therefore, at 1500K and 1600K no potassium compounds formed and only the cement portion of the sample was detected.

The 71% alumina cement-sodium listed in Table 5 shows the appearance of sodium aluminate and $C_{12}A_7$ at all temperatures tested. The thermodynamic calculations predict the formation of sodium aluminate throughout the temperature range tested.⁽¹⁰⁾ The lime phase disappears between 1500K and 1600K. The ternary compound, $N_2C_3A_5$ first appears at 1400K.

The 71% alumina cement-potassium phases listed in Table 6 confirm the theoretical calculations up to 1600K, with the formation of lime and potassium aluminate. At 1600K, the loss of potassium during testing prevented the formation of potassium aluminate.

It should be noted that the formation of the high molar ratio (1:1) alkali-aluminates was a direct result of the excess amounts of alkali impurities used during testing. A 1:1 weight ratio of alkali carbonates to alumina cement was used to promote reaction in the relatively short testing period of 30 hours. At low alkali levels, beta-alumina will form above 2000°F and will be stable up to 3000°F. The formation of beta-alumina will result in a 20% volume increase.

Table 5. Calculated Equilibrium Phases and the Experimentally Observed Phases for the Sodium-71% Alumina Cement Reactions

Temperature (K)	Calculated	Observed
1200	C, NA	$C_{12}A_7$, NA
1300	C, NA	$C_{12}A_7$, NA, C
1400	C, NA	$C_{12}A_7$, NA, C, $N_2C_3A_5$
1500	C_3A , CA, NA	$C_{12}A_7$, NA, C, $N_2C_3A_5$
1600	CA, NA	$C_{12}A_7$, NA, $N_2C_3A_5$

Table 6. Calculated Equilibrium Phases and the Experimentally Observed Phases for the Potassium-71% Alumina Cement Reactions

Temperature (K)	Calculated	Observed
1200	C, KA	$C_{12}A_7$, KA, C
1300	C, KA	$C_{12}A_7$, KA, C
1400	C, KA	$C_{12}A_7$, KA, C
1500	C, KA	$C_{12}A_7$, KA, C
1600	C, KA	CA, CA_2

B. Solubility Results

The solubility curves of sodium aluminate and potassium aluminate are shown in Figures 4 and 7, respectively. Both curves increase with increasing temperatures and begin to level off at 90°C to 100°C, where steam will begin to first appear. In a steam containing atmosphere, approximately 9.0g/L of sodium aluminate or potassium aluminate was soluble. The solubility curve for $N_2C_3A_5$ (see Figure 5) levels off at 50°C and remains constant up to 100°C; over this temperature range 3.1g/L was soluble. The solubility curve for nepheline (see Figure 6) increases with increasing temperature but shows no tendency to level off. In a steam containing atmosphere only 1.1g/L of nepheline was soluble. Kaliophilite was the least soluble of the alkali compounds tested. For all practical purposes, kaliophilite was insoluble at 5°C (0.025g/L). The solubility curve for kaliophilite shown in Figure 8 also increases with increasing temperature without leveling off. At 90°C, only 0.70g/L of kaliophilite was soluble.

C. Thermal Expansion Results

The thermal expansion curves for sodium aluminate and nepheline (Figures 9 and 11, respectively) have a constant slope from 300°C to 800°C. The slope of the thermal expansion curves is defined as the coefficient of thermal expansion. The slope of the thermal expansion curve is constant from 200°C to 800°C for $N_2C_3A_5$ (see Figure 10). The slope of the thermal expansion curve for potassium aluminate (Figure 12) increases nonlinearly with increasing temperature. A constant coefficient of thermal expansion can not be assumed over the temperature range from room temperature to 800°C. The coefficient of thermal

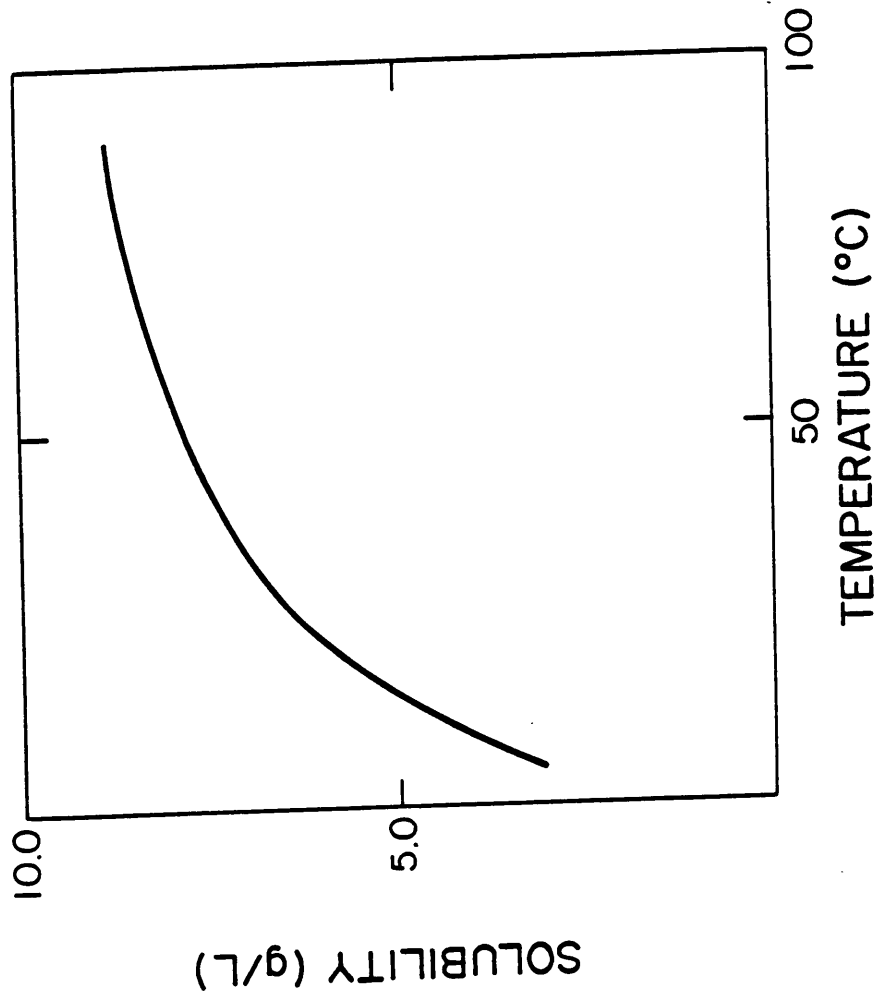


Figure 4. Solubility Curve for Sodium Aluminate

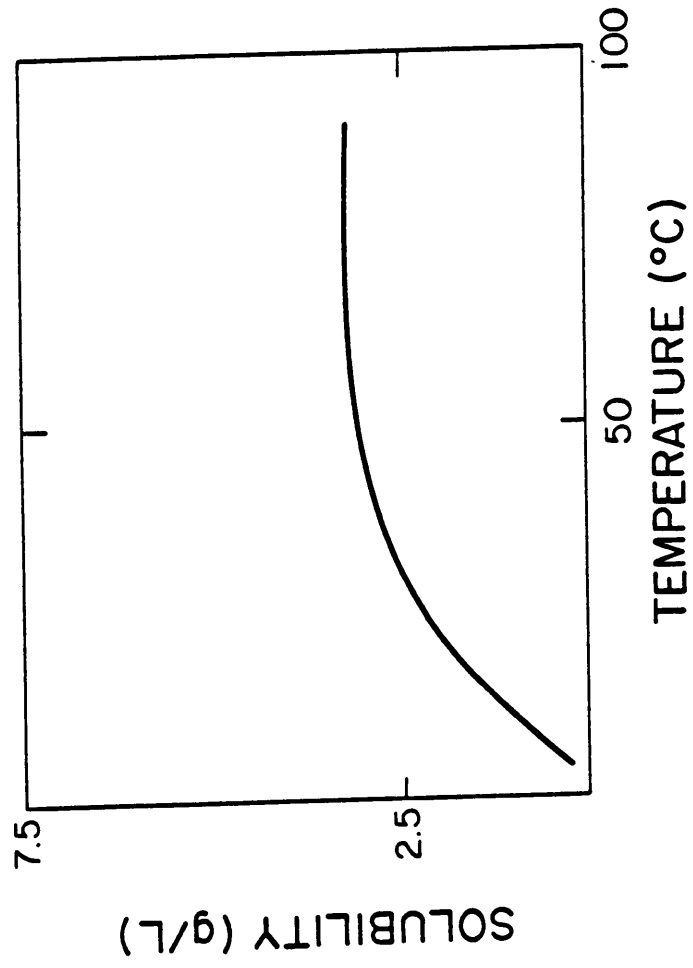


Figure 5. Solubility Curve for Soda-Lime-Aluminate

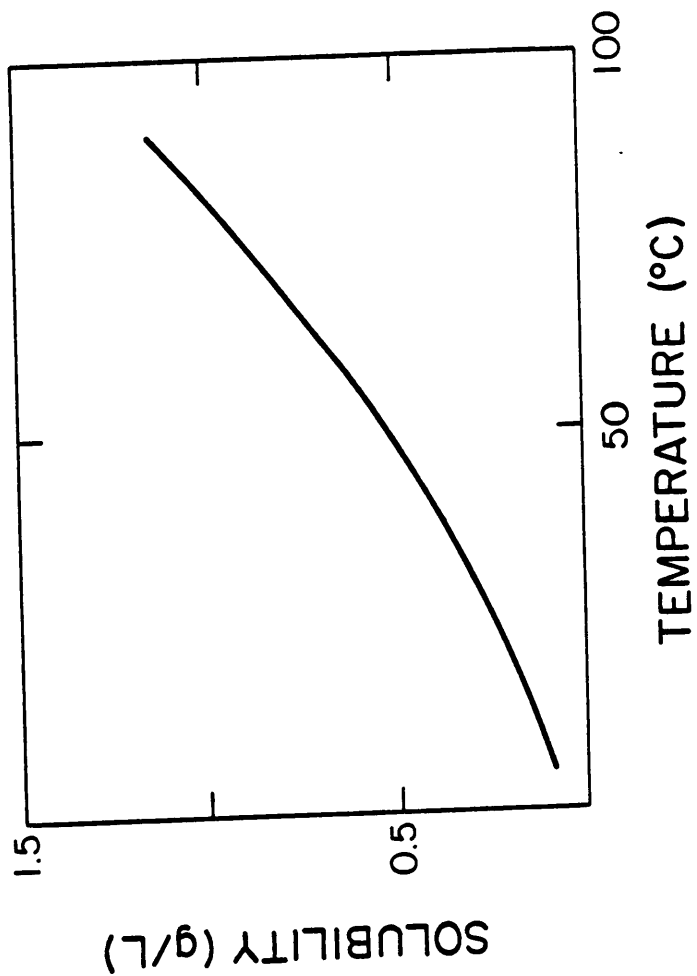


Figure 6. Solubility Curve for Nepheline

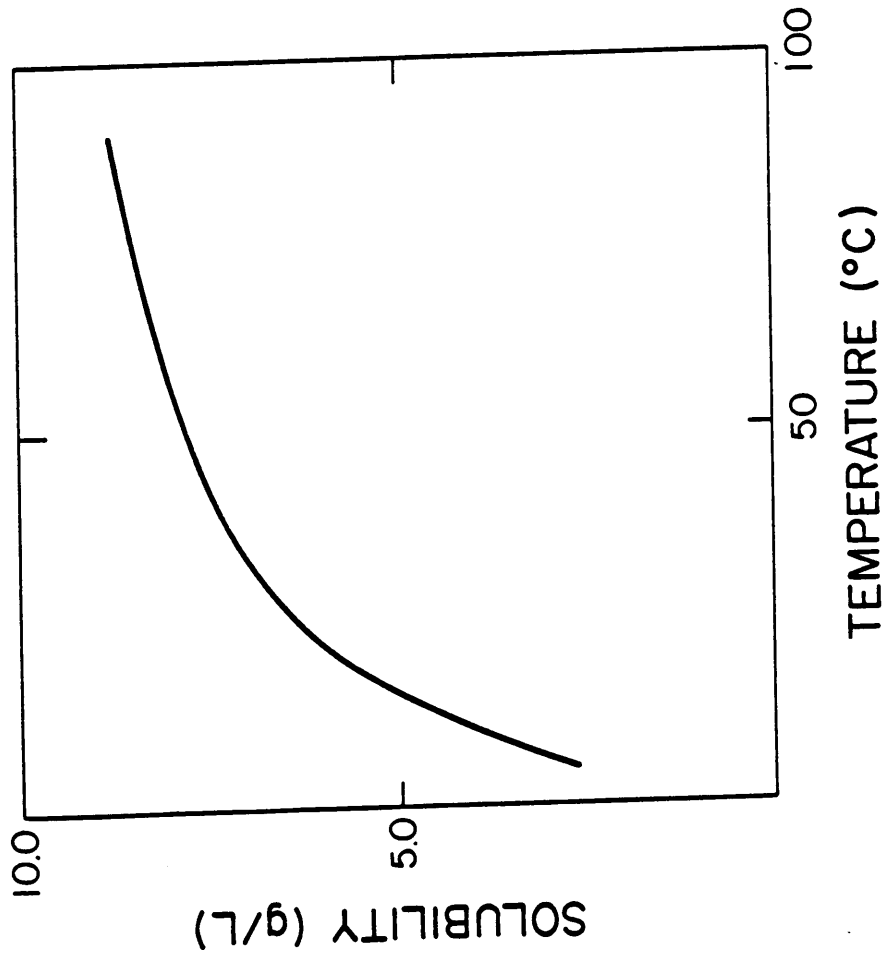


Figure 7. Solubility Curve for Potassium Aluminate

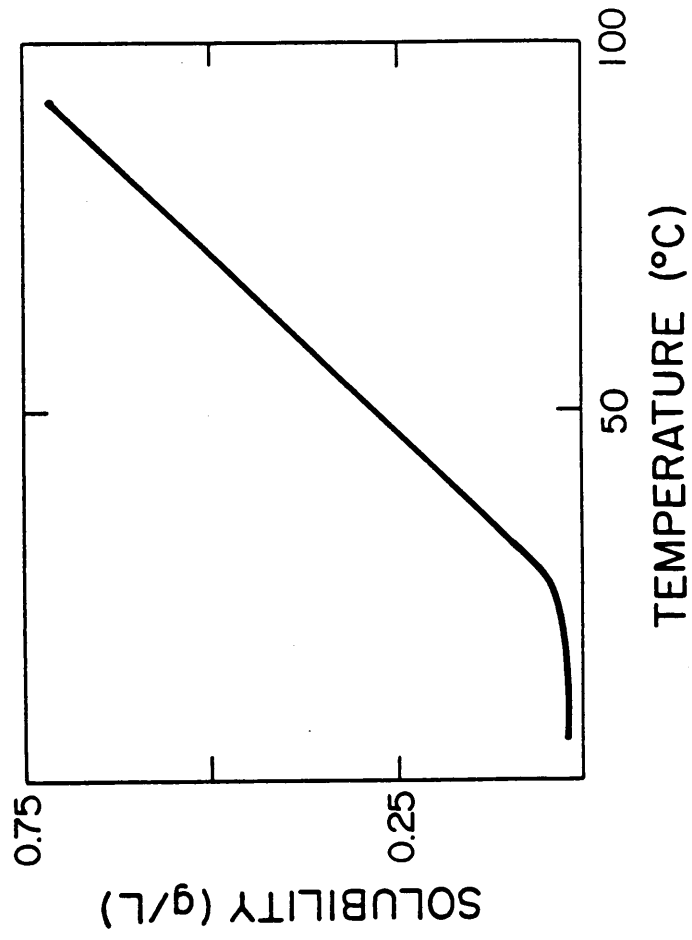


Figure 8. Solubility Curve for Kaliophillite

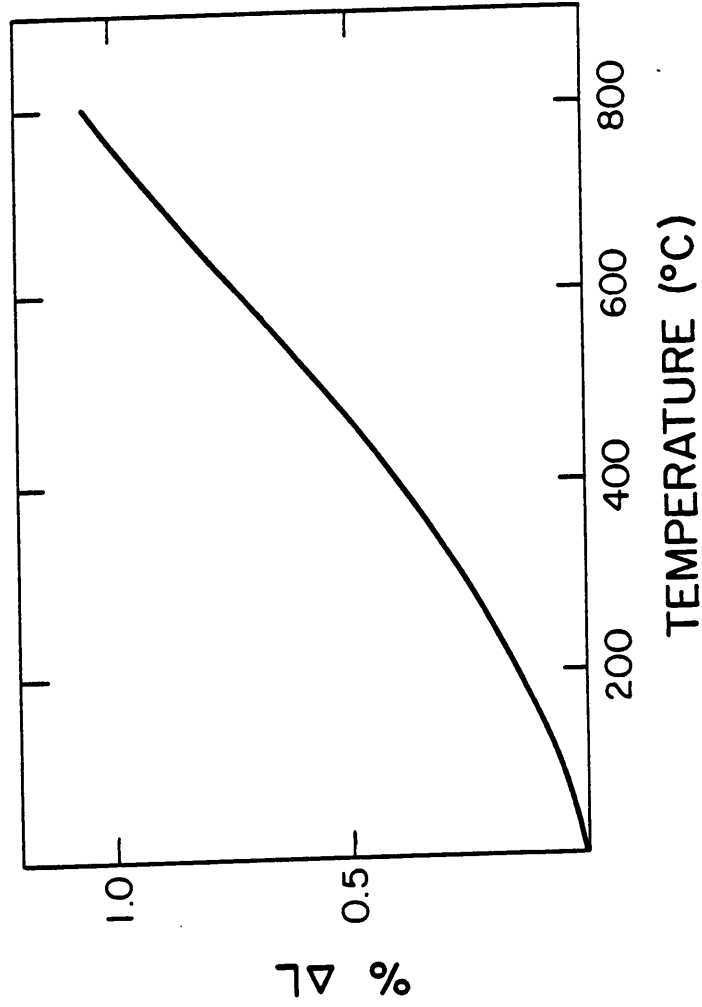


Figure 9. Thermal Expansion Curve for Sodium Aluminate

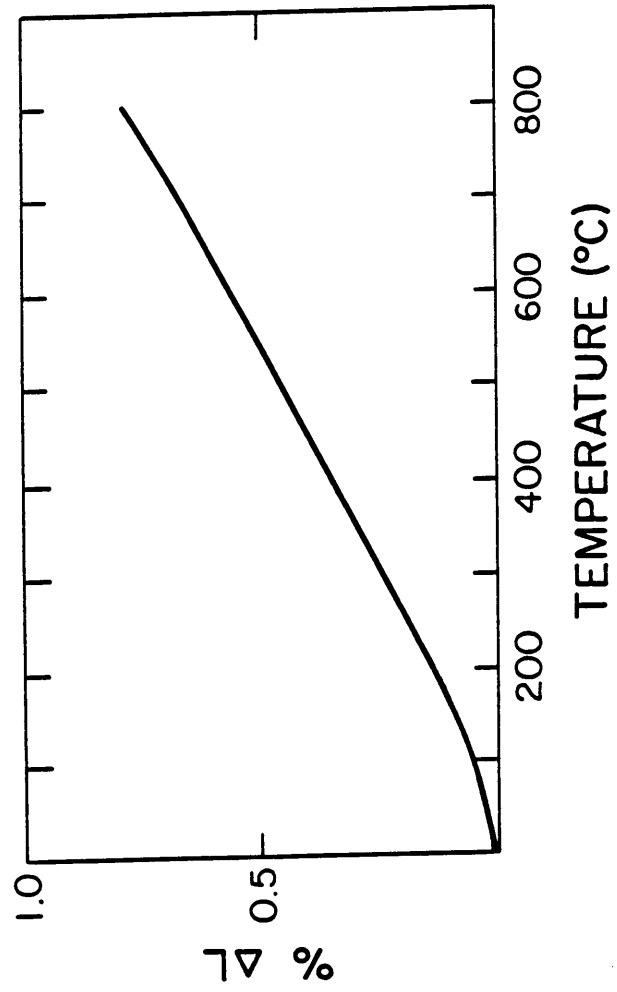


Figure 10. Thermal Expansion Curve for Soda-Lime-Aluminate

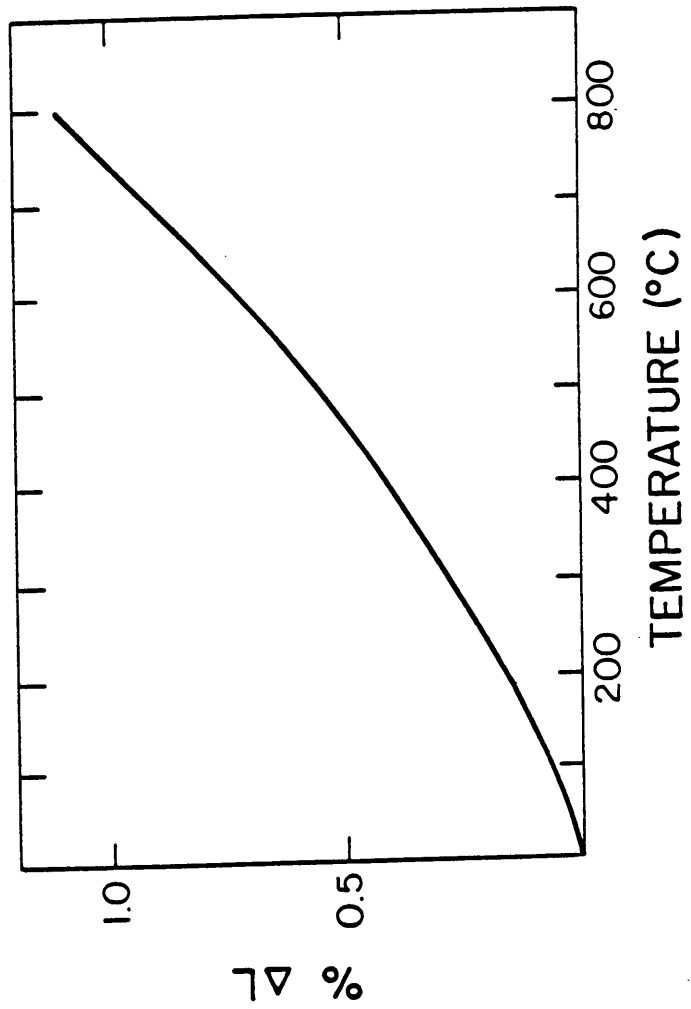


Figure 11. Thermal Expansion Curve for Nepheline

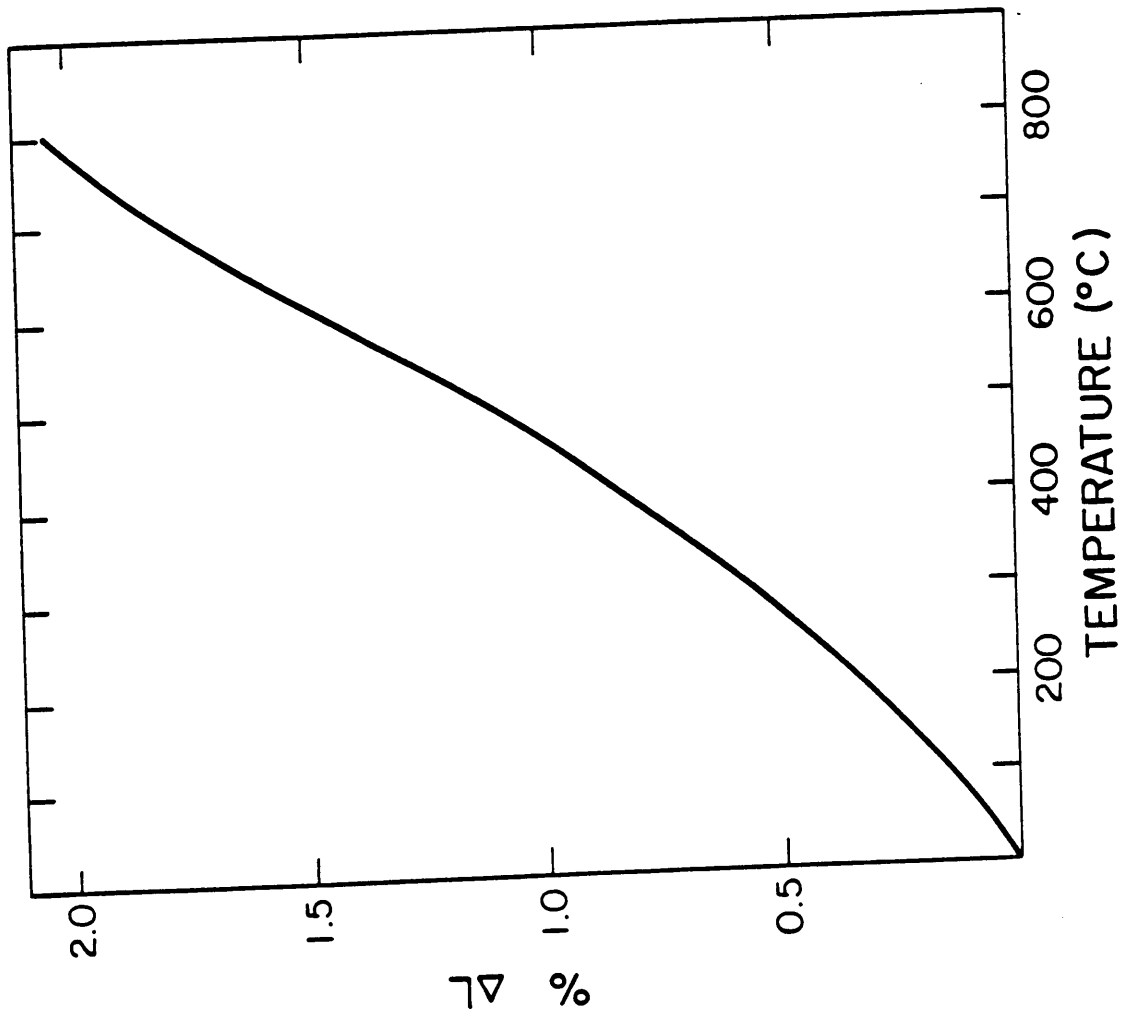


Figure 12. Thermal Expansion Curve for Potassium Aluminate

expansion of potassium aluminate was the largest of the reported values given in Table 7. Heating potassium aluminate from room temperature to 800°C would result in 2.05% linear expansion. The thermal expansion curve for kaliophilite is shown in Figure 12. The slope also increases nonlinearly with increasing temperature. Therefore, a constant coefficient of thermal expansion can not be assumed for kaliophilite. A linear expansion of 1.48% can be expected when kaliophilite is heated from room temperature to 800°C.

D. Discussion

If the presence of the alkali impurities cannot be avoided by changes in the operating conditions or coal, then the rate of alkali attack must be retarded. The attack mechanism of alkali on aluminous refractories is impregnation, bond reaction, and bond depletion. As previously stated, the sequence of alkali attack is initially the glass and cristobalite phases, then the mullite and finally the alumina. Resistance to alkali attack by aluminous refractories was characterized by Farris and Allen as follows⁽¹⁸⁾: for aluminous refractories of 50 percent or less alumina, the refractory microstructure must be mature and have low surface area, low porosity, and low alkali content. For aluminous refractories containing 50 percent alumina and higher, the matrix mullite bond should be mature and of minimum exposed surface area. The matrix should also have minimum glass and cristobalite, and should be of low alkali content. Maturity of the matrix bond and minimum surface area are important aspects of alkali resistance. They appear to be as important as the refractory composition.

Table 7. Coefficients of Linear Thermal Expansion of the Tested Alkali Compounds

Alkali Compounds	$\alpha \times 10^{-6}$ in/in/ $^{\circ}\text{C}$
Sodium Aluminate (NA)	14.05
Nepheline (NAS_2)	14.20
Soda-Lime-Aluminate ($\text{N}_2\text{C}_3\text{A}_5$)	9.75
Potassium Aluminate (KA)	27.75
Kaliophilite (KAS_2)	22.35

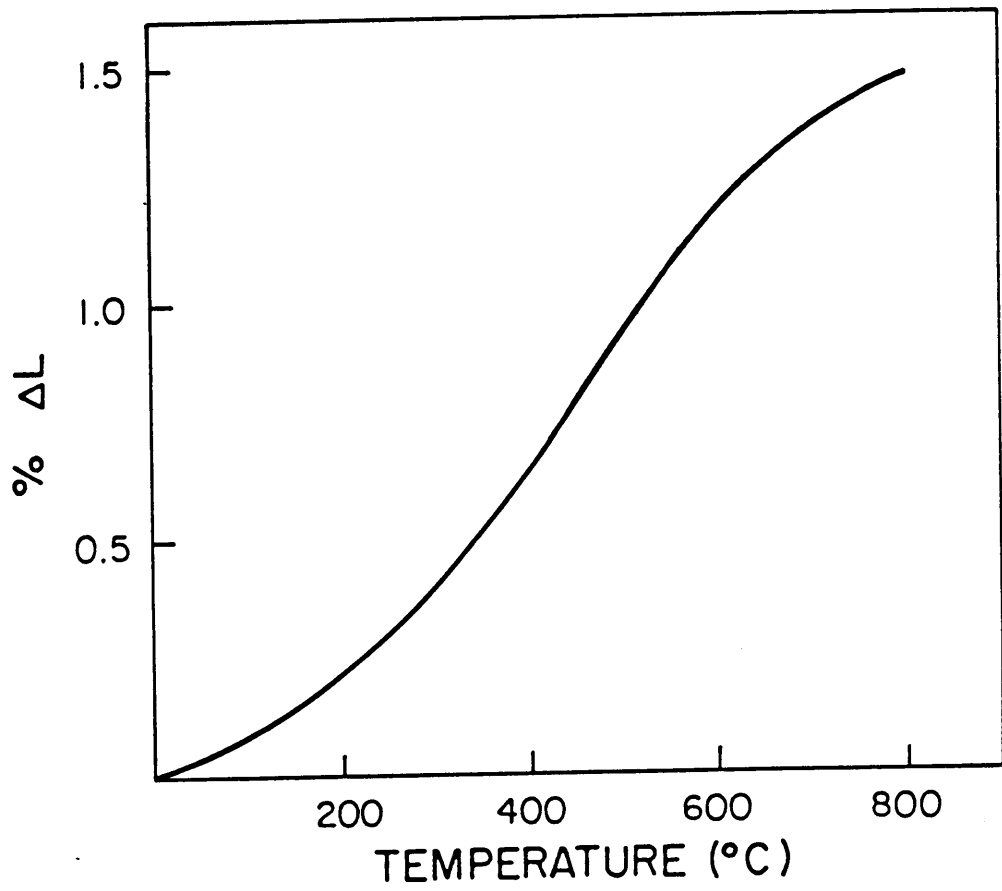


Figure 13. Thermal Expansion Curve for Kaliophilite

From a refractory selection standpoint, superduty fireclay refractories can be used as long as the maximum hot-face temperature does not exceed 1000°C . The hot-face would show a volume contraction at temperatures below 1000°C and melting would occur above 1000°C . As the temperature is increased, the alumina content must be increased. Sillimanite could be used up to 1300°C and pure alumina brick beyond 1600°C without appreciable fluxing of the hot-face. At lower temperatures both of these bricks would show an expansive tendency at the hot-face.

Since alkali impurities are almost always present in coal processing, the formation of the dry expansive compounds is inevitable. By estimating the amount of alkali present in the coal feed and monitoring the operating temperature of the gasifier, the relative amounts of the alkali compounds which will form can be calculated. The coefficients of thermal expansion of the alkali compounds can then be used to calculate the percent linear expansion which will occur upon heating of the refractory lining to a specified temperature. These calculations can be used to estimate the life of the refractory lining.

From a design viewpoint, improving the cooling system will minimize the solubility of the alkali compounds. Lowering the solubility of the alkali compounds will result in less moisture removal when the gasifier is cooled to ambient conditions and subsequently reheated. Effective lowering of the operating temperature will also lead to less damage of the refractory lining by reducing the amount of thermal expansion and the subsequent spalling. The phase beta-alumina could also be designed into the refractory to tie up all the free alumina. This would prevent

further reaction between the alkali impurities and the refractory lining. The large volume expansion associated with the beta-alumina phase occurs only upon formation. After the initial volume expansion, subsequent heating of beta-alumina would produce a coefficient of thermal expansion comparable to corundum.

IV. Conclusions

The experimental results confirmed the formation of sodium aluminate ($\text{Na}_2\text{O} \cdot \text{Al}_2\text{O}_3$), soda-lime-alumina ($2\text{Na}_2\text{O} \cdot 3\text{CaO} \cdot 5\text{Al}_2\text{O}_3$), and potassium aluminate ($\text{K}_2\text{O} \cdot \text{Al}_2\text{O}_3$) predicted by thermodynamic calculations. These compounds along with nepheline ($\text{Na}_2\text{O} \cdot \text{Al}_2\text{O}_3 \cdot 2\text{SiO}_2$) and kaliophilite ($\text{K}_2\text{O} \cdot \text{Al}_2\text{O}_3 \cdot 2\text{SiO}_2$) were synthesized and characterized according to their solubility in water and linear thermal expansion. The water solubility at 90°C of sodium aluminate and potassium aluminate was approximately 9.0g/L for both samples; they were found to be the most soluble of the compounds tested. The solubility of the ternary compound, $\text{N}_2\text{C}_3\text{A}_5$, was 3.1g/L. The solubility at 90°C of nepheline was 1.1g/L. Kaliophilite was the least soluble with only 0.7g/L being soluble at 90°C .

The linear thermal expansion of sodium aluminate and nepheline was found to be 1.1% from room temperature to 800°C . Over the same temperature range, $\text{N}_2\text{C}_3\text{A}_5$ expanded only 0.57%. The linear thermal expansion of kaliophilite was 1.48% from room temperature to 800°C . The thermal expansion of potassium aluminate was the highest at 2.05% from room temperature to 800°C . Of the compounds tested, the formation of potassium aluminate would be the most detrimental to the gasifier lining. The thermal expansion of potassium aluminate was twice as large as the other compounds and it possessed the highest solubility in water.

V. References

1. C.R. Kennedy, "Alkali Attack on a Mullite Refractory in the Grand Forks Energy Technology Center Slagging Gasifier," J. Materials for Energy Systems, Vol. 3, p.28, June, 1981.
2. R.E. Farris and J.E. Allen, "Aluminous Refractories-Alkali Reactions," Iron and Steel Engineer, p.68, Feb., 1973.
3. Ibid.
4. R.C. DeVries and W.L. Roth, "Critical Evaluation of the Literature Data on Beta Alumina and Related Phases: Phase Equilibria and Characterization of Beta Alumina Phases," Journal of American Ceramic Society, Vol. 52, No.7, p.364, July 1969.
5. Raymond Ridgeway, Albert Klein and W.J. O'Leary, "The Preparation and Properties of So-Called Beta Alumina," Trans. Electrochem. Soc., Vol.70, p.71, 1936.
6. Yamaguchi and Suzuki, "On the Structure of Alkali Polyaluminates," Bulletin of the Chemical Society of Japan, Vol. 41, p.93, 1968.
7. G. Rigby and R. Hutton, "Action of Alkali and Alkali-Vanadium Oxide Slags on Alumina-Silica Refractories," J. Amer. Cer. Soc., Vol. 45, February, p.70, 1962.
8. C.R. Kennedy, "Alkali Attack on a Mullite Refractory in the Grand Forks Energy Technology Center Slagging Gasifier," J. Materials for Energy Systems, Vol. 3, p.29, June, 1981.
9. P.H. Havranek, "Alkali Attack on Blast Furnaces Refractories," Trans. J. Brit. Ceram. Soc., Vol. 77, p.93, 1978.
10. Tawei Sun, Master's Thesis, Virginia Polytechnic Institute and State University, June, 1986.
11. F.M. Lea, The Chemistry of Cement and Concrete, p.72, Edward Arnold Publishers Ltd., 1970.
12. M.S. Beletskii and Yu.G. Saksonov, "X-ray Diffraction Studies of Polymorphic Transformations in Sodium Aluminate," Russian Journal of Inorganic Chemistry, Vol. 4, No.5, p.442, May, 1959.
13. J.V. Smith and O.F. Tuttle, "The Nepheline-Kalsilite System: X-ray Data for the Crystalline Phases," Amer. J. Sci., Vol. 255, p.283, April, 1957.
14. A.F. Reid and A.E. Ringwood, "High-Pressure NaAlO_2 , an α - NaFeO_2 Isotype," Inorganic Chemistry, Vol. 7, p.444, 1968.

15. Borchert and Keidel, Heidelberger Beitr. Mineral U Petrog., Vol. 1, pp.17-30, 1949.
16. Hughes, "Formation of Alkali Silicates and Alumino-Silicates and Their Occurrence in Blast Furnaces," Trans. Brit. Cer. Soc., Vol. 65, p.662, 1966.
17. R.P. Meyer, M.J. and R.R. Brown, "Thermodynamic Properties of $KAlO_2$," J. Chem. Thermodynamics, Vol. 12, pp.985-991, 1980.
18. R.E. Farris and J.E. Allen, "Aluminous Refractories-Alkali Reactions," Iron and Steel Engineer, p.74, Feb., 1973.

Appendix I

Table 1. Solubility of Sodium Aluminate in Water

	<u>Solubility (g/L)</u>		
	5°C	25°C	90°C
	3.11	5.83	8.80
	3.11	6.02	8.81
	3.15	5.92	8.73
	3.17	5.85	8.76
(average)	3.14	5.91	8.78

Table 2. Solubility of Potassium Aluminate in Water

	<u>Solubility (g/L)</u>		
	5°C	25°C	90°C
	2.58	6.03	8.83
	2.60	6.04	9.02
	2.59	6.00	8.89
	2.59	5.96	8.81
(average)	2.59	6.00	8.89

Table 3. Solubility of $N_2C_3A_5$ in Water

	<u>Solubility (g/L)</u>		
	5°C	25°C	90°C
	0.420	2.16	3.17
	0.372	2.14	3.17
	0.305	2.16	3.16
	0.350	2.19	3.19
(average)	0.362	2.16	3.17

Table 4. Solubility of Nepheline in Water

	<u>Solubility (g/L)</u>		
	5°C	25°C	90°C
	0.104	0.219	1.09
	0.082	0.219	1.18
	0.098	0.181	1.20
	0.091	0.209	1.16
(average)	0.094	0.207	1.16

Table 5. Solubility of Kaliophilite in Water

	<u>Solubility (g/L)</u>		
	5°C	25°C	90°C
	0.027	0.030	0.69
	0.027	0.031	0.74
	0.027	0.032	0.70
	0.020	0.032	0.67
(average)	0.025	0.031	0.70

Appendix II

Table 1. Thermal Expansion of Sodium Aluminate

Temperature °C	Decimal ($\Delta l/l_0$) in/in	(%)
23	0	0
100	0.0005	0.05
200	0.0015	0.15
300	0.0026	0.26
400	0.0041	0.41
500	0.0057	0.57
600	0.0073	0.73
700	0.0090	0.90
800	0.0105	1.05

Table 2. Thermal Expansion of Nepheline

Temperature °C	Decimal ($\Delta l/l_0$) in/in	(%)
23	0	0
100	0.0005	0.05
200	0.0017	0.17
300	0.0030	0.30
400	0.0044	0.44
500	0.0058	0.58
600	0.0073	0.73
700	0.0092	0.92
800	0.0112	1.12

Table 3. Thermal Expansion of $N_2C_3A_5$

Temperature °C	Decimal ($\Delta l/l_0$) in/in	(%)
23	0	0
100	0.0003	0.03
200	0.001	0.10
300	0.0018	0.18
400	0.00255	0.255
500	0.00338	0.338
600	0.0042	0.42
800	0.0057	0.57

Table 4. Thermal Expansion of Potassium Aluminate

Temperature °C	Decimal ($\Delta l/l_0$) in/in	(%)
23	0	0
100	0.00105	0.105
200	0.0032	0.320
300	0.00555	0.555
400	0.00825	0.825
500	0.01115	1.115
600	0.01465	1.465
700	0.01795	1.795
800	0.02045	2.045

Table 5. Thermal Expansion of Kaliophilite

Temperature °C	Decimal ($\Delta l/l_0$) in/in	(%)
23	0	0
100	0.0007	0.07
200	0.0023	0.23
300	0.0039	0.39
400	0.00645	0.645
500	0.009175	0.9175
600	0.011725	1.1725
700	0.013725	1.3725
800	0.0148	1.48

**The vita has been removed from
the scanned document**